The aging skin microenvironment dictates stem cell behavior

Yejing Ge[a,b,1,2], Yuxuan Miao[a,b], Shiri Gur-Cohen[a,b], Nicholas Gomez[a,b], Hanseul Yang[a,b], Maria Nikolova[a,b], Lisa Polak[a,b], Yang Hu[c], Akanksha Verma[c], Olivier Elemento[c], James G. Krueger[d], and Elaine Fuchs[a,b,2]

[a]Robin Neustein Laboratory of Mammalian Development and Cell Biology, The Rockefeller University, New York, NY 10065; [b]Howard Hughes Medical Institute, The Rockefeller University, New York, NY 10065; [c]Department of Physiology and Biophysics, Caryl and Israel Englander Institute for Precision Medicine, Institute for Computational Biomedicine, Weill Cornell Medicine, New York, NY 10065; and [d]Laboratory for Investigative Dermatology, The Rockefeller University, New York, NY 10065

Contributed by Elaine Fuchs, January 21, 2020 (sent for review February 8, 2019; reviewed by Angela M. Christiano, Angela L. Tyner, Amy J. Wagers, and Rui Yi)

Aging manifests with architectural alteration and functional decline of multiple organs throughout an organism. In mammals, aged skin is accompanied by a marked reduction in hair cycling and appearance of bald patches, leading researchers to propose that hair follicle stem cells (HFSCs) are either lost, differentiate, or change to an epidermal fate during aging. Here, we employed single-cell RNA-sequencing to interrogate aging-related changes in the HFSCs. Surprisingly, although numbers declined, aging HFSCs were present, maintained their identity, and showed no overt signs of shifting to an epidermal fate. However, they did exhibit prevalent transcriptional changes particularly in extracellular matrix genes, and this was accompanied by profound structural perturbations in the aging SC niche. Moreover, marked age-related changes occurred in many nonepithelial cell types, including resident immune cells, sensory neurons, and arrector pili muscles. Each of these SC niche components has been shown to influence HF regeneration. When we performed skin injuries that are known to mobilize young HFSCs to exit their niche and regenerate HFs, we discovered that aged skin is defective at doing so. Interestingly, however, in transplantation assays in vivo, aged HFSCs regenerated HFs when supported with young dermis, while young HFSCs failed to regenerate HFs when combined with aged dermis. Together, our findings highlight the importance of SC:niche interactions and favor a model where youthfulness of the niche microenvironment plays a dominant role in dictating the properties of its SCs and tissue health and fitness.

aging | stem cells | lineage identity | skin | hair follicle

Adult stem cells (SCs) undergo long-term self-renewal and multilineage differentiation (1, 2) and are responsible for maintaining tissue homeostasis and repairing wounds. Irrespective of usage frequency, SCs endure increasingly strained demands to maintain tissue integrity over the course of a lifetime of repeated environmental insults. Initially viewed as the long-sought fountain of youth, SCs in aging tissues do not have an endless functional output, and inevitably tissue fitness wanes (3–11). What accounts for this age-related decline in SC activity remains unclear. Increasing evidence from young adult tissues points to the importance of the SC niche (i.e., its tissue microenvironment) as a key modulator of SC behavior. Thus, in order to identify the drivers of aging, and devise interventions that prolong adult SC function and improve age-related tissue fitness, it will be necessary to interrogate not only the aging SCs, but also their niche.

Murine skin represents an excellent model to tackle this important problem. During embryogenesis, skin epithelium begins as a single layer of unspecified progenitors, which progressively give rise to the stratified layers of the epidermis and its appendages, including hair follicles (HFs), sebaceous, sweat, and mammary glands. As morphogenesis proceeds, SCs and progenitors are set aside in discrete niches, each of which then instructs their residents what to do and when (12–16).

In adult skin, HFSCs reside in an anatomical niche called the bulge (17), where they fuel the synchronized, cyclical bouts of quiescence (telogen), active hair growth (anagen), and destruction (catagen). Just above the bulge is the attachment site of the arrector pili muscle (APM), which thermoregulates by controlling the positioning of the hairs relative to the body surface. Also located above the bulge are four different types of sensory neurons that enable perception of touching or stroking of the hair coat. During the quiescent period, the dermal papilla (DP) resides directly below the bulge. Prolonged cross-talk between the DP and adjacent HFSCs is needed to enter the hair growth phase. Additional inputs from the lymphatic capillaries, adipose tissue, dermal fibroblasts, immune cells (e.g., macrophages and regulatory T cells), and HFSC progeny themselves have all been reported to impact HFSC behavior, and participate in the transition from resting state to active HF regeneration and hair growth (18–29). The lymphatic network also integrates the activity of HFSCs across the tissue (28).

In normal homeostasis of young mice, each new hair cycle begins when positive signals from various niche inputs override inhibitory cues, prompting HFSCs to regenerate the lower two-thirds

Significance

Adult tissues harbor tissue-specific stem cells (SCs), essential for wound repair and fitness. Organ deterioration is often attributed to loss or lineage-skewing of these resident SCs. Using murine skin, we combine single-cell RNA-sequencing with functional studies to examine age-related changes of hair follicle (HF) SCs and their microenvironment ("niche") that together govern hair regeneration. Surprisingly, aged HFSCs decrease but retain their fate and remain undifferentiated. However, they exhibit altered extracellular matrix gene expression that correlates with a decline in hair regeneration following wounding. Interestingly, aged SCs can be rejuvenated if combined with neonatal dermis in transplantation assays, but even young SCs are not similarly supported by aged dermis. These findings underscore the importance of altered SC microenvironment in driving skin aging.

Author contributions: Y.G. and E.F. designed research; Y.G., Y.M., S.G.-C., M.N., and L.P. performed research; Y.G. and J.G.K. contributed new reagents/analytic tools; Y.G., N.G., H.Y., Y.H., A.V., and O.E. analyzed data; and Y.G. and E.F. wrote the paper.

Reviewers: A.M.C., Columbia University; A.L.T., University of Illinois College of Medicine; A.J.W., Harvard University; and R.Y., University of Colorado Boulder.

The authors declare no competing interest.

Data deposition: The data reported in this paper have been deposited in the Gene Expression Omnibus (GEO) database, https://www.ncbi.nlm.nih.gov/geo (accession no. GSE124901).

[1]Present address: Department of Cancer Biology, MD Anderson Cancer Center, University of Texas, Houston, TX 77054.

[2]To whom correspondence may be addressed. Email: yge1@mdanderson.org or fuchslb@rockefeller.edu.

This article contains supporting information online at https://www.pnas.org/lookup/suppl/doi:10.1073/pnas.1901720117/-/DCSupplemental.

First published February 24, 2020.

of the HF and grow hair. In response to a partial-thickness wound, HFSCs are also mobilized to re-epithelialize the missing tissue in the interfollicular epidermis and in the upper HF, including the sebaceous glands (19, 30–38). In transit, they adopt certain features of the stem cells of these new tissues, while retaining characteristics of the HFSCs, a phenomenon that we've referred to as "lineage infidelity" (35). Once the wound is healed, however, this transient state is resolved, and HFSCs take on the identity characteristic of the destination-resident SCs whose niches they have now adopted. Such broadening of lineage choices is similarly observed when HFSCs are taken from their native niche and engrafted into foreign hosts in transplantation studies (39, 40). Together, these findings illustrate the impact of the niche on SC behavior in homeostasis and wound healing.

Less clear is how changes in the niche impact SC activity and lineage choices in the skin later in life. Age-related declines in SC activity and tissue fitness have been described for both epidermis (41–43) and HFs (44–48), and in many cases, the role of aging tissue microenvironment has been implicated (24, 41, 42, 44, 46, 47, 49, 50). The relation between changes in the aging niche and lineage choices of the SCs remains unclear. Curiously, age-related skewing of SC lineage choices or precocious differentiation has been noted in other tissues (51–54). In this regard, aging HFSCs have been suggested to undergo epidermal conversion, thereby accounting for the age-related miniaturization of HFs and paucity of hairs (48). In contrast to wound repair, however, where young HFSCs undergo fate switching upon taking up a new niche residence (35), an age-related switch in SC fate within their native niche would imply that either there is an intrinsic fate plasticity in SCs that becomes unstable with age, or that the niche has been modified in an age-related manner to promote such skewing of fates.

In the present study, we sought to explore these possibilities by characterizing the multifaceted phenotypic and molecular changes that take place in aged HFSCs and their surrounding tissue microenvironment. Unexpectedly, we discovered that HFSCs within their aged niche maintain lineage identity, and show little evidence of epidermal conversion. While remaining faithful in their lineage identity, aged HFSCs displayed clear changes in the expression of extracellular matrix (ECM) genes, and these perturbations were accompanied by distinct structural alterations within the bulge niche. Also notable were marked age-related changes in the nonepithelial components of the dermal microenvironment that are known to impact HFSC behavior. Correspondingly, we found that aging skin is severely compromised in its ability to regenerate HFs following an injury, a feature that relies not only upon SC function, but also contributions from the surrounding dermis. Finally, we show that these extrinsic stimuli largely override the intrinsic differences displayed by young and aged HFSCs. Thus, neonatal dermal cells rejuvenate aged HFSCs during in vivo transplantations, while aged dermal cells fail to support even young HFSCs under such circumstances. Overall, our findings point to the importance of the tissue microenvironment as a key functional determinant of SC aging.

Results

HFSCs in Aged Skin Maintain their Lineage Identity. We began by investigating age-related transcriptome changes within the skin epithelium of 2-y-old (aged) and 2-mo-old (young) C57BL/6 mice (*SI Appendix*, Fig. S1). Because the hair cycle of the aged murine hair coat is more asynchronous than younger mice (46, 47), we focused on back skin HFs in their resting (telogen) stage. After dissecting the epithelium from the skin, we used FACS to remove dead cells and further exclude immune cells, melanocytes, fibroblasts, and endothelial cells. We then captured single cells enriched for skin epithelial lineages and performed single-cell RNA-sequencing (scRNA-seq) using the 10X Genomics platform (*Materials and Methods*).

Unsupervised clustering and visualization with *t*-distributed stochastic neighbor embedding (tSNE) revealed distinct telogen-phase cell populations from both young and aged skin epithelium (Fig. 1*A*). We used established lineage-specific markers to distinguish the identities of the following populations: Bulge HFSCs, "primed" HFSCs at the bulge base (hair germ, HG), sebaceous glands, isthmus (the HF region between the bulge and sebaceous glands), infundibulum (the upper HF region contiguous with the epidermis), suprabasal HF cells, and basal and suprabasal cells of the epidermis (Fig. 1*B* and *SI Appendix*, Fig. S1).

Overall, the cellular patterns of young and aged epithelia were strikingly similar, providing little hints of age-related blurring of cellular states. Notably, bulge HFSCs formed a unique cluster seen in both young and aged skin, and when the data from the two groups were combined, they were comparable in tSNE and split-dot plots (Fig. 1 *A* and *B*). Additionally, aged bulge HFSCs displayed no major reductions in key HF identity transcripts nor did they show signs of induction of epidermal genes (Fig. 1*C*).

Given the absence of new intermediate or transitional states based on single cell transcriptomic analysis, we next addressed whether aged HFSCs may have shifted completely to an epidermal fate within the bulge niche. To test this possibility, we performed immunofluorescence with known bulge and epidermal lineage markers. Like their younger counterparts, aged HFSCs maintained bulge SC identity genes, such as KERATIN 24 (K24) (Fig. 2*A*) and SOX9 (Fig. 2*B*) (41, 44, 46). Additionally, we did not observe ectopic induction of either KLF5, an epidermal SC marker (Fig. 2*B*), or KERATIN 10 (K10), an epidermal fate and differentiation marker (Fig. 2*C* and *SI Appendix*, Fig. S2*A*). Overall, overt signs of SC fate-switching or epidermal differentiation within the bulge itself were missing.

To complement our approaches of scRNA-seq and immunofluorescence, we employed FACS to purify young and aged HFSCs and interfollicular epidermal SCs (EpdSCs). We then used conventional bulk RNA-seq to compare their transcriptomes, and also assay for transposase-accessible chromatin with high-throughput sequencing (ATAC-seq) to compare their accessible chromatin profiles (*Materials and Methods*). As expected from our scRNA-seq data, principal component analysis (PCA) showed that bulge HFSCs from both young and aged skin clustered closely, and differed markedly from young and aged EpdSCs, which also clustered tightly (Fig. 2*D*). Further analyses revealed that consistent to transcriptional profiles, accessible chromatin patterns for key bulge and EpdSC genes differed based upon SC type, rather than age (Fig. 2*E*). Taken together, at least in their resting state, we find that bulge HFSCs appeared to be remarkably faithful in maintaining cell identity during aging.

Aged HFSCs Display Pronounced Changes in ECM Gene Expression and in Bulge Structure. Although aged bulge HFSCs were faithful in their identity, a number of changes distinguished aged transcriptomes from their younger counterparts. Most notably, the top significantly changed transcripts from gene ontology (GO) term analysis of bulk RNA-seq were ECM, basement membrane, ECM-remodeling genes, and secreted signaling factors (Fig. 3 *A* and *B*, *SI Appendix*, Fig. S2*B*, and Datasets S1 and S2).

Seeking the possible significance of these findings, we were drawn to the marked baldness in regions of aged murine skin (Fig. 3*C*). Although the degree of hair loss varied significantly, the sparse hair coat was intriguing, given that HFSCs were still present in the aging bulge niches without showing signs of epidermal conversion or differentiation. Upon closer inspection at the level of whole-mount immunofluorescence microscopy, we identified several distinct structural differences between the young and aged bulge.

Specifically, young HFs in the second telogen (i.e., second postnatal resting phase of the hair cycle) exhibited a well-defined, two-bulge structure (Fig. 3*D*). As noted previously (25), at this stage one bulge was active, distinguished by a discernable HG,

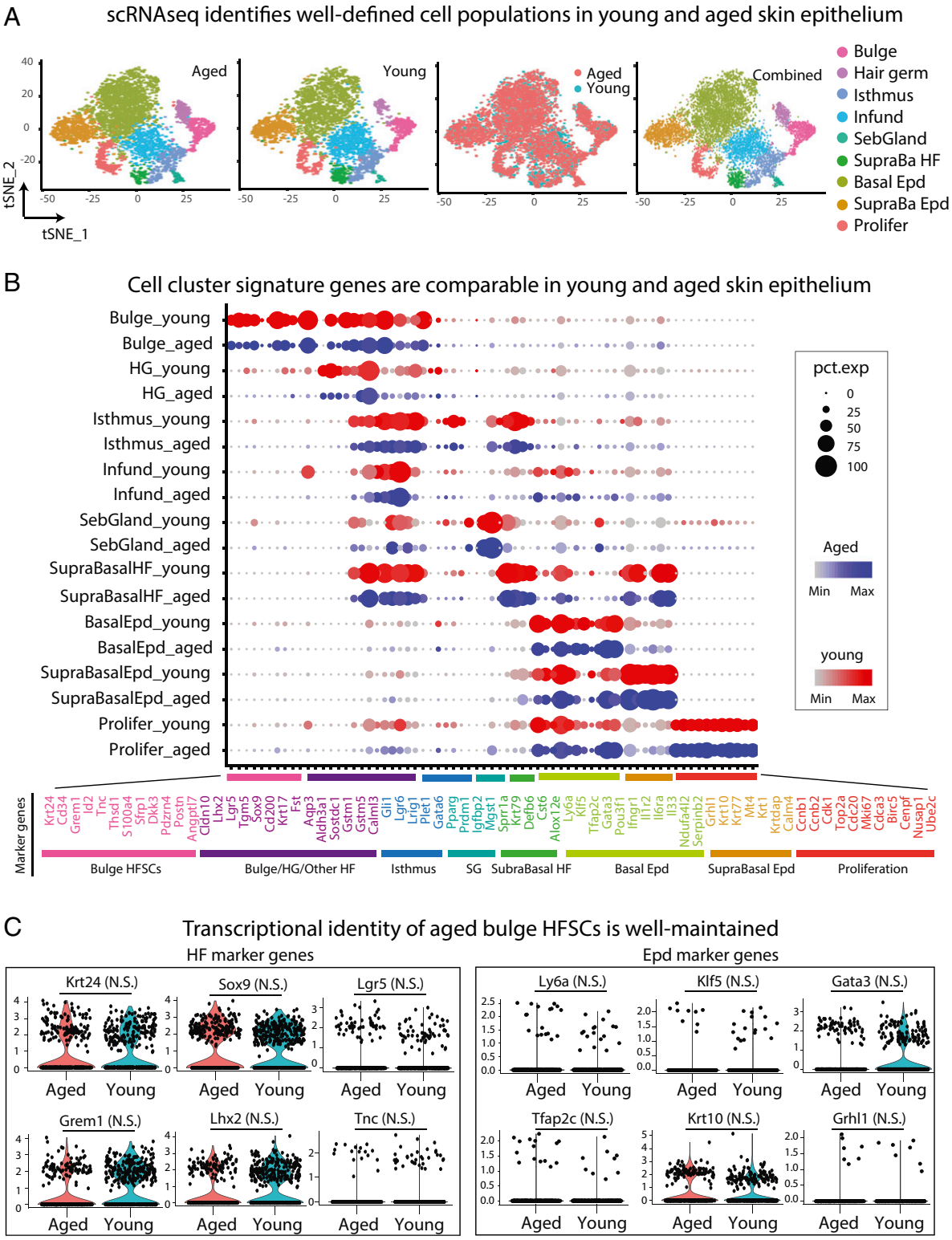

Fig. 1. scRNA-seq analysis suggest that bulge HFSCs in the aged skin maintain their lineage identity. scRNA-seq was performed on purified epithelial cells from the back skins of young (2 mo) and aged (24 mo) mice (*Materials and Methods*). (*A*) tSNE plots show similar patterns of cell clustering for young and aged skins. (*B*) Split dot-plots show that each cell cluster stratifies according to known lineage and identity markers. Each circle is a gene, with size representing percentage of cells expressing this gene and color representing expression level (see annotation to the right, blue = aged, red = young). The *x* axis lists gene names and cell identity; the *y* axis lists cluster assignments. (*C*) Violin plots of HF and epidermal (Epd) marker genes expressed by young and aged bulge HFSCs. These cells were defined by clustering and signature expression. Note that there are no detectable changes in the expression of marker genes. N.S., not significant.

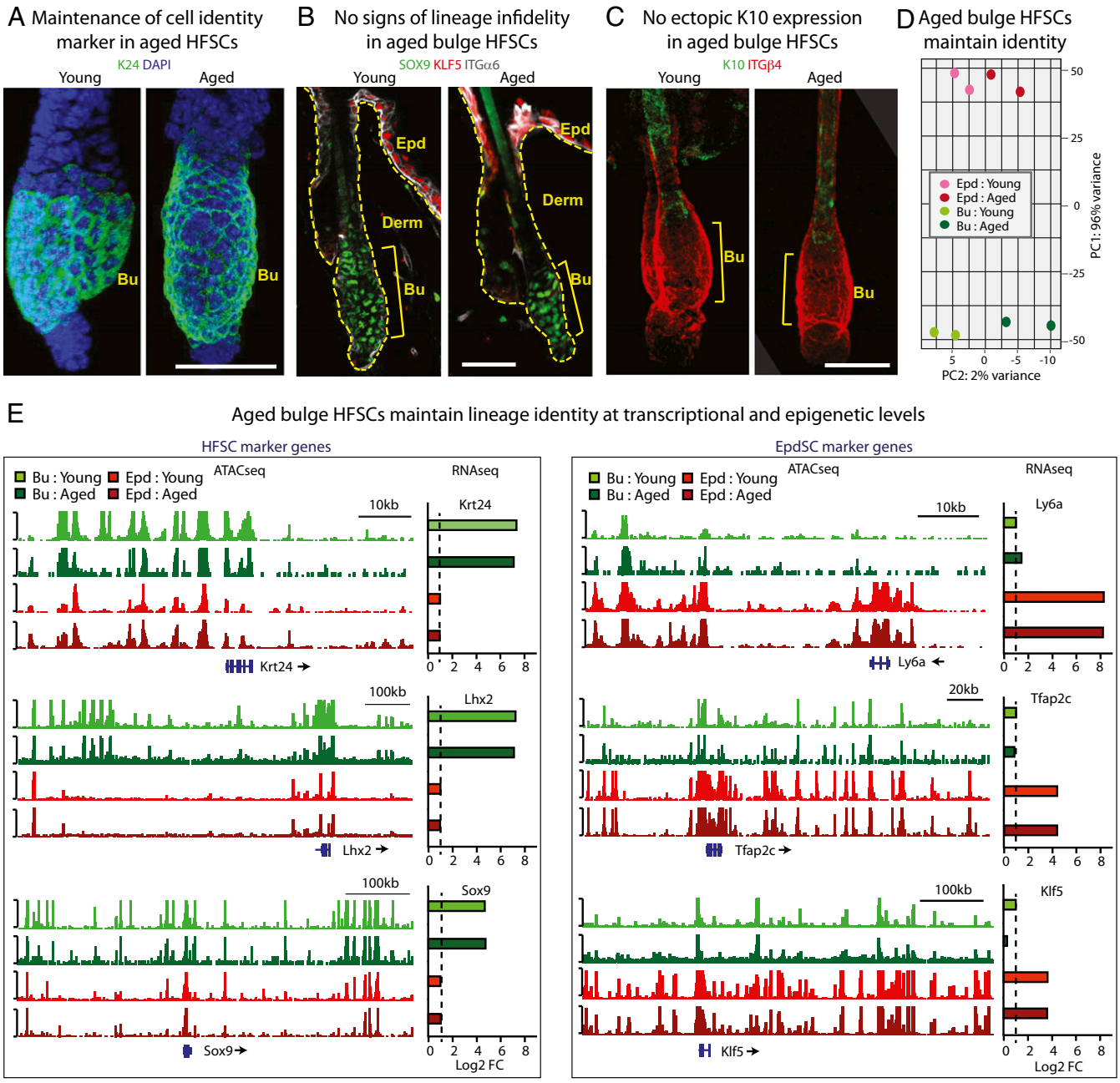

Fig. 2. During the hair cycle resting stage, aged bulge HFSCs maintain their lineage identity. (*A–C*) Immunofluorescence of HFSC markers K24 (*A*) and SOX9 (*B*), and EpdSC marker KLF5 (*B*), and Epd differentiation marker K10 (*C*). Bu, bulge; Derm, dermis; Epd, epidermis; ITGα6, INTEGRIN α6; ITGβ4, INTEGRIN β4. At least five independent biological replicates were performed; shown are representative images. (Scale bars, 30 μm.) (*D*) PCA on bulk RNA-seq of aged versus young bulge HFSCs (green) and EpdSCs (red) further suggest that aged bulge HFSCs do not convert to an EpdSC-like fate. Data are from two biologically independent replicates. (*E*) ATAC-seq tracks show accessible chromatin regions of genes transcribed in: HFSCs (*Krt24, Lhx2, Sox9*) and EpdSCs (*Ly6a* [=*Sca1*], *Tfap2c* [=*AP2g*], *Klf5*), and how their patterns differ in young versus aged bulge HFSCs (green) and EpdSCs (red). Bulk RNA-seq $\log_2$ fold-change values (dashed line shows the baseline) are plotted next to ATAC-seq tracks, showing specific expression of HFSC and EpdSC identity genes, respectively.

(primed HFSCs), essential for hair cycling, while the other was inactive and anchored the hair from the previous hair cycle (known as the "club hair"). In contrast, aged HFs often displayed only a single bulge (Fig. 3*D*), a phenotype highly penetrant regardless of hairy or bald (Fig. 3 *D* and *E* and Movies S1–S3).

This phenotype was particularly notable, considering that by 2 y of age, mice had undergone eight to nine hair cycles, potentially adding one bulge with each cycle (55, 56). It is known that the inactive bulge only persists until the club hair from the previous hair cycle is lost, at which time it merges with the single, active bulge (25, 56). Consistently, the severity of hair loss correlated with the prevalence of the single-bulge phenotype (Fig. 3 *C* and *E*). Additionally, an age-related reduction in HFSCs was particularly noticeable in mice with accentuate balding (*SI Appendix*, Fig. S2*C*), consistent with a collapsed bulge structure and HF miniaturization during aging. Once bald, these skin regions did not appear to spontaneously resume hair growth, at least under unperturbed conditions. Moreover, since single-housed animals maintained baldness, these phenotypic changes were not attributable to grooming.

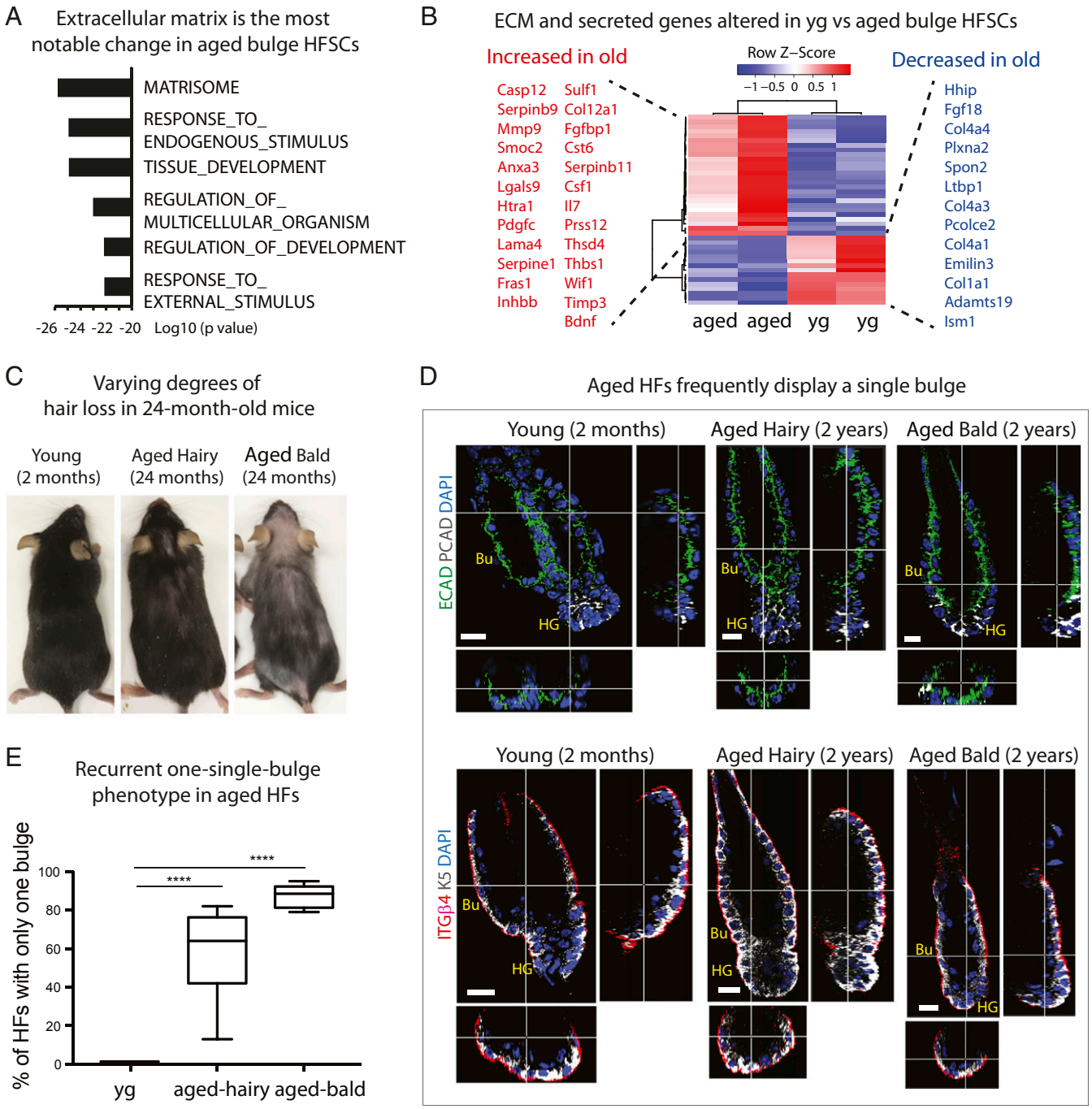

Fig. 3. Age-related changes in the HFSC transcriptome and bulge structure point to ECM perturbations in the niche. (*A*) GO term analysis on bulk RNA-seq. Note that the top changed category between young and aged HFSCs is matrisome (ECM genes). Note also marked changes in endogenous and exogenous stimuli. (*B*) Heatmap showing hierarchical clustering of ECM genes and secreted factors that are significantly changed between aged and young HFSCs. Red, increased expression; blue, decreased expression. (*C*) Examples of variability in hair loss phenotype displayed by aged (24-mo-old) C57BL/6 mice. (*D*) Whole-mount immunofluorescence of telogen-phase HFs labeled for E-CADHERIN (ECAD) and P-CADHERIN (PCAD) (*Upper*), and K5 and INTEGRIN β4 (ITGβ4) (*Lower*). Images of vertical and horizontal planes (crossbars) are shown at the right and bottom of each main frame, respectively. Note that young HFs display the expected two-bulge structure, but aged HFs show only a single bulge, regardless of whether hairy or bald. Bu, bulge; HG, hair germ. At least five independent biological replicates were analyzed; shown are representative images. (Scale bars, 10 μm.) (*E*) Quantifications of data shown in *D*. $n = 5$. Data are presented as mean ± SEM. Paired *t* test was performed, $^{****}P < 0.0001$.

Also notable was that in the hairy aged skin, the single bulge was still associated with an HG at this point, consistent with their potential ability to generate new hairs (Fig. 3*D*). In contrast, in bald aged skin, the HG was markedly diminished. These observations suggested that despite the presence of HFSCs within aged HF bulges, they might be largely inert. This is consistent with a previous report that aged HFSCs are more sluggish in activating and initiating the new hair cycle (46). Indeed, these aged bulges appeared to be in a resting state, indicated by lack of Ki67 immunostaining therein (*SI Appendix*, Fig. S2*D*). Consistent with their quiescent state, cell cycle gene expression remained relatively constant and low

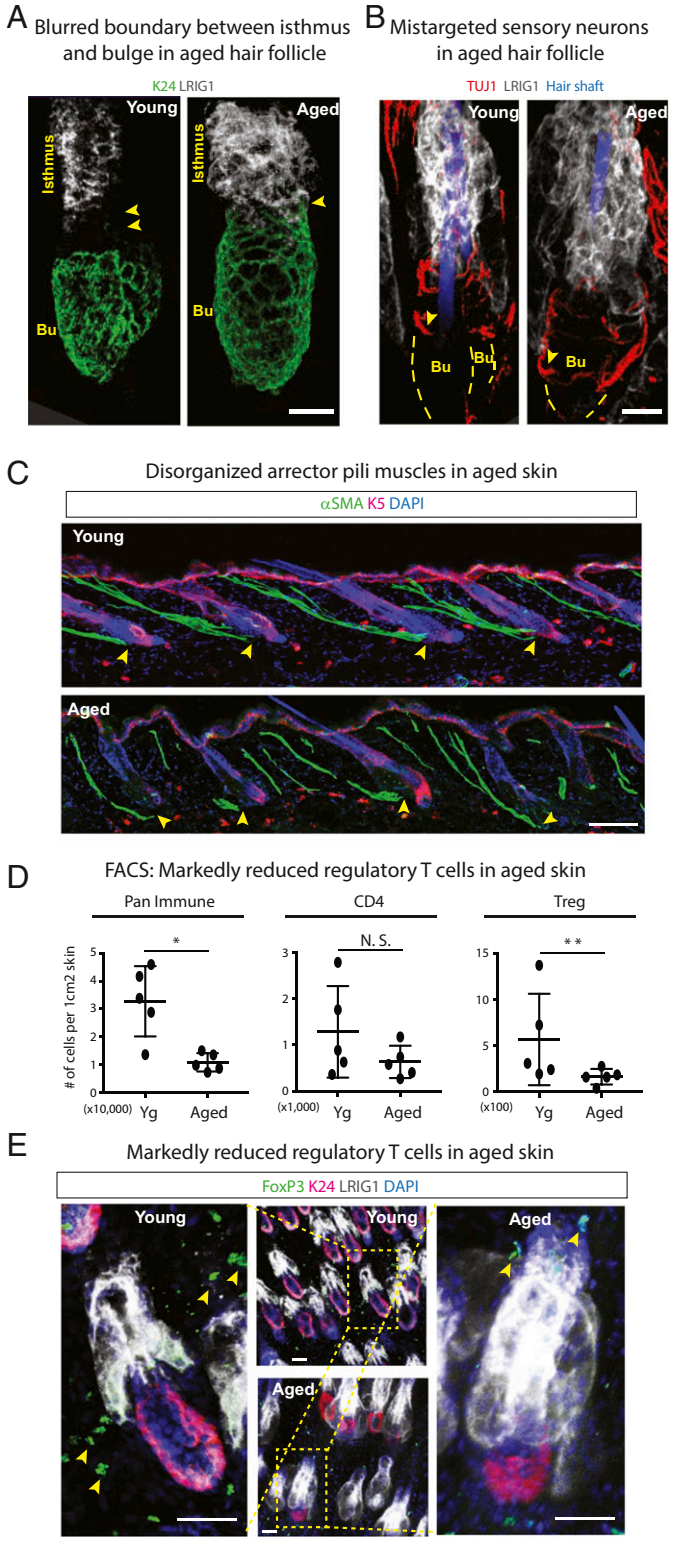

Fig. 4. Multifaceted changes in the aged skin microenvironment. (*A* and *B*) Whole-mount immunofluorescence of telogen-phase young and aged HFs immunolabeled for HFSC marker K24, isthmus marker LRIG1, and sensory neuronal marker TUJ1. Arrowheads in *A* point to the spatial separation between the bulge (Bu) and isthmus. In young HFs, this zone harbors the four sensory neurons that wrap around the HFs. In aged HFs, this zone is missing. Arrowheads in *B* show that sensory neurons have relocalized to the bulge in aged HFs. (Scale bars, 20 μm.) (*C*) Immunofluorescence of α-smooth muscle actin (αSMA) in young and aged skin reveals that APMs lose their anchorage (arrowheads) to the bulge in aged skin. (Scale bar, 50 μm.) (*D*) FACS analysis of skin resident immune cell populations showing age-related reductions in $CD45^+$ pan-immune populations, no significant change in the overall cohort of $CD4^+$ effector T cells, but specific reductions in $CD4^+FOXP3^+CD25^+$ Tregs. $n = 5$. Data are presented as mean ± SEM. Paired *t* test was performed, $^*P < 0.05$, $^{**}P < 0.01$, N.S., not significant. (*E*) Whole-mount immunofluorescence of telogen-phase young and aged HFs immunolabeled for HFSC marker K24, isthmus marker LRIG1, and Treg marker FOXP3. Arrowheads in *E* point to the $FoxP3^+$ Treg cells in the young and aged skin. (Scale bars, 30 μm.) For *A*–*C* and *E*, at least five independent biological replicates were analyzed. Shown are representative images.

across young and aged HFSC cohorts at this time (*SI Appendix*, Fig. S2*E*).

Altogether, aging bulge HFSCs were reduced in numbers and those present appeared inert but transcriptionally active, exhibiting marked alterations in expression of the ECM and ECM-remodeling genes. These alterations correlated with the inability of their bulge niches to maintain structural integrity, a phenomenon that may underlie HF miniaturization in aged skin. Intriguingly, such age-related HF miniaturization was reminiscent of previously characterized genetic models of alopecia (56, 57), and it will be interesting in the future to examine whether similar structural alterations might be converging between natural aging and pathological states.

Multifaceted Changes in the Aged Skin Microenvironment. Irrespective of the precise mechanisms underlying age-related hair sparseness, aging HFSCs maintained their lineage identity, and remained nonproliferative during the resting phase of the hair cycle. However, the marked changes in ECM gene expression by HFSCs and structural alterations in the SC niche suggested that perturbations in the microenvironment might be involved in the age-related decline of HFSC activity. In this regard, we were intrigued by recent studies reporting striking functional differences between aged dermal fibroblasts and their young counterparts (20, 21, 23, 24, 49). To obtain a further understanding of the age-related differences in the HFSC microenvironment, we surveyed additional nonepithelial cell types that have been implicated as HFSC niche components (18, 19, 22).

One particularly notable change came from coimmunolabeling for the bulge HFSC marker K24 and for LRIG1, a marker for the isthmus of the HF. In young follicles, there is normally a gap between the two HF regions, corresponding to the position where the sensory neurons typically reside (19). In contrast, the $LRIG1^+$ isthmus was contiguous with the aged bulge (Fig. 4*A*). Furthermore, upon labeling for the sensory neurons, it was clear that rather than wrapping around the region between bulge and isthmus, they were mis-targeted, extending downward around the bulge (Fig. 4*B*, arrowheads, and Movies S4 and S5). Accompanying this mislocalization was an age-dependent elevation in transcripts encoding *Bdnf* (Fig. 3*B*), a well-known neuronal growth factor (58).

Another striking change in the aged bulge niche was the APM. Normally, the APM connects to the HF at the upper bulge (18), but in the aged skin, the APM appeared to be detached from the bulge (Fig. 4*C*). APM attachment is dependent upon a specialized ECM component, nephronectin (NPNT), expressed by the SCs in young bulges (18). Notably, although not reaching statistical significance, a consistent trend was seen toward *Npnt* downregulation in aged versus young HFSCs (Datasets S1 and S2). That said, with the myriad of age-related differences in ECM gene expression, multiple perturbations might together contribute to the age-related differences we observed in APM attachment.

Previously, we reported significant age-related perturbations in the cross-talk between EpdSCs and dendritic epidermal T cells (DETCs), which reside within the epidermis and serve as important immune response sentinals for pathogens that enter wounded

skin (42). Focusing here on dermal immune changes that might affect bulge HFSC behavior, we observed a significant reduction in total immune cell numbers in aged skin (Fig. 4*D*) (pan-immune). Moreover, although changes in the overall $CD4^+$ effector T cell population were not as significant (42), clear age-related reductions were found in the subset of regulatory T cells (Tregs) within this pool (Fig. 4 *D* and *E*). The age-related diminished numbers of $FOXP3^+CD25^+CD4^+$ Tregs were particularly noteworthy in light of a recent report that in young mice, Tregs have a stimulatory effect on hair cycling (22). Thus, the paucity of Tregs could be a significant contributor to the age-related decline in hair cycling.

When taken together with the age-related transcriptomic alterations in HFSCs, the distinct changes in the aged bulge niche and HF microenvironment provide insights into why the hair coat becomes sparser with age and why hair cycling wanes despite the presence of HFSCs in aged skin. Each of these age-related changes we identified in SC:niche interactions could directly or indirectly contribute to SC functional decline during skin aging.

Defective HF Regeneration in Aged Skin during Wound Repair. Previously, we reported that when aged epidermal SCs are challenged to re-epithelialize the epidermis in a full-thickness wound, the repair process is markedly delayed (42). Here, we turned to a partial-thickness dremel wound model where the epidermis and upper portion of HFs are removed, leaving the bulge HFSCs beneath the wound bed to become the main drivers of the re-epithelialization process (*Materials and Methods* and Fig. 5*A*). In this situation, the mobilized HFSCs enter a lineage infidelity state (35), driving epidermal repair. Additionally, in young mice, the stress response induced by partial thickness wounding stimulates HF regeneration, making the model a particularly attractive one to challenge the potency of the aged HFSCs (Fig. 5*A*).

To better monitor hair regrowth, we first shaved telogen-phase young and aged mice, and then performed partial thickness wounding on their back skin. For both young and aged mice, unwounded regions flanking the wound site remained in the resting stage 2 wk postwounding (Fig. 5*B*, areas demarcated by white dotted lines; Fig. 5 *C*, *Lower*). In contrast, only in young and not aged mice, hair growth was evident within re-epithelialized skin. In young re-epithelialized skin, visible hairs were present at the wound site, and skin acquired a black appearance, reflecting the pigmented hairs of mature follicles beneath the skin surface (Fig. 5*B*, areas demarcated by yellow dotted lines in the young). However, aged skin in repaired wound regions lacked visible hairs and remained pale (Fig. 5*B*, areas demarcated by yellow dotted lines in the aged).

Closer inspection revealed that bulges were still intact following this wound procedure administered to both young and aged skins (*SI Appendix*, Fig. S3*A*). Additionally, soon after wounding, both young and aged HF bulges initiated a hair cycle. In striking contrast to young skin, however, most HFs failed to mature fully and produce hair (Fig. 5 *C*, *Upper*).

Even at 2 mo postinjury, when the unwounded region of young mice had now launched its normal hair cycle (Fig. 5*D*, white dotted lines in young, Fig. 5*E*, "unwounded young"), the aged skin still showed no signs of regenerating a new hair coat, regardless of being wounded or unwounded (Fig. 5 *D* and *E*, aged). Additionally, even though wounded HFs in the aged skin had begun to regenerate during the first 2 wk of wound repair, they had now gone back to a resting state (Fig. 5*E*, "wounded aged").

The age-related defect in hair regeneration seemed to be at odds with the previous notion that aged resting skin resembles a chronic wound-like state (41, 50, 59). Since HFSCs were still present in the aging HF bulges within balding skin regions (Fig. 1) and were induced to activate hair cycling upon wounding (Fig. 5*C*), we surmised that either the aged HFSCs and their early proliferative progenies were defective in their ability to execute the hair regenerative program, or they might be short of sustainability, grinding their tissue regenerative task to a halt.

Seeking deeper understanding, we examined earlier steps in the wound-repair process. Five days postwounding, aged HFSCs appeared to have launched tissue repair (*SI Appendix*, Fig. S3*B*). At this time, the epidermis and upper portion of HFs both showed signs of tissue regeneration (*SI Appendix*, Fig. S3*B*, arrowheads). These findings indicate that aged HFSCs were still able to respond to the wound-induced cues that galvanize epidermal re-epithelialization. Additionally, wound-responsive aged HFSCs that had left their bulge niche expressed both epidermal (KLF5) and HF (SOX9) transcription factors, classic signs of lineage infidelity (*SI Appendix*, Fig. S3*C*, arrows). This state is essential for wound repair (35).

In addition to initiating these features of wound repair, aged HFSCs were also able to activate a number of steps along the normal path to follicle maturation and hair production (Fig. 6*A*). Like their youthful counterparts, HFs displayed *Shh* and *Wnt10b*, which are critical markers of the early short-lived SC progenies in the hair bulb that fuel HF regeneration and hair growth (60) (magnified boxed insets in Fig. 6*A*, arrowheads). That said, although molecular signals for regeneration were initiated, by 7 d postwounding, regenerated aged HFs appeared shorter, a reflection of presumably fewer outer root sheath cells that harbor the SCs for the next hair cycle (26). HFs were also less mature, a reflection of fewer short-lived HFSC progeny in the hair bulb that will progress to differentiate into the hair shaft and its channel (inner root sheath) (61). Indeed, many aged follicles lacked a hair shaft, which in young C57BL/6 mice was clearly recognizable by the melanin pigment that hair cells take up during the terminal differentiation process (Fig. 6*A* arrows, and Fig. 6*B* quantification). Correspondingly, aged follicles displayed diminished numbers of $GATA3^+$ inner root sheath lineage cells, and fewer $HOXC13^+$ hair shaft lineage cells (arrowheads in Fig. 6 *C* and *D*, respectively). Ki67 immunolabeling further revealed that within each of the progenitor pools that fuel HF regeneration and differentiation, proliferation was markedly diminished in aged follicles (Fig. 6*E*). This was true for outer root sheath progenitors (Fig. 6*E*, arrowheads) as well as hair bulb progenitors (Fig. 6*E*, brackets).

Taking these data together, we find that aging HFSCs responded to wound-induced anagen-promoting cues, and produced proliferating progenies that appeared capable of executing their proper lineage differentiation pathways. However, they were compromised in their capacities to sustainably fuel regeneration throughout the hair cycle. In turn, this led to the inability to regenerate the hair coat in aged mice subjected to partial thickness wounds.

Intrinsic Differences between Young and Aged HFSCs Can Be Overridden by In Vitro Culture. A priori, the poor capacity of aged HFSCs in wound-induced tissue regeneration could be due either to intrinsically diminished activity of the HFSCs, or to the poorly supportive tissue microenvironment provided by the aged dermis. To begin to distinguish between these possibilities, we first isolated HFSCs from young and aged skin, and monitored their behavior in vitro (*SI Appendix*, Fig. S4*A*). When SCs are taken outside their native niche, they often undergo a stress response (16, 62), a process analogous to wound repair in vivo (35, 63). Of note, such stress is reversible in young HFSCs, and when transplanted back into mice, they resolve the stress and give rise to all lineages of HFs and epidermis (39, 64).

Indeed, like their younger counterparts, aged HFSCs underwent transcriptional changes in culture that were similar to those seen during wound repair (35), including 1) activation of epidermal genes, 2) down-regulation of HF genes, and 3) induction of stress-specific genes (*SI Appendix*, Fig. S4*B*). The ability of aged HFSCs to recapitulate the lineage infidelity state in vitro was in good agreement with our earlier in vivo observation that aged

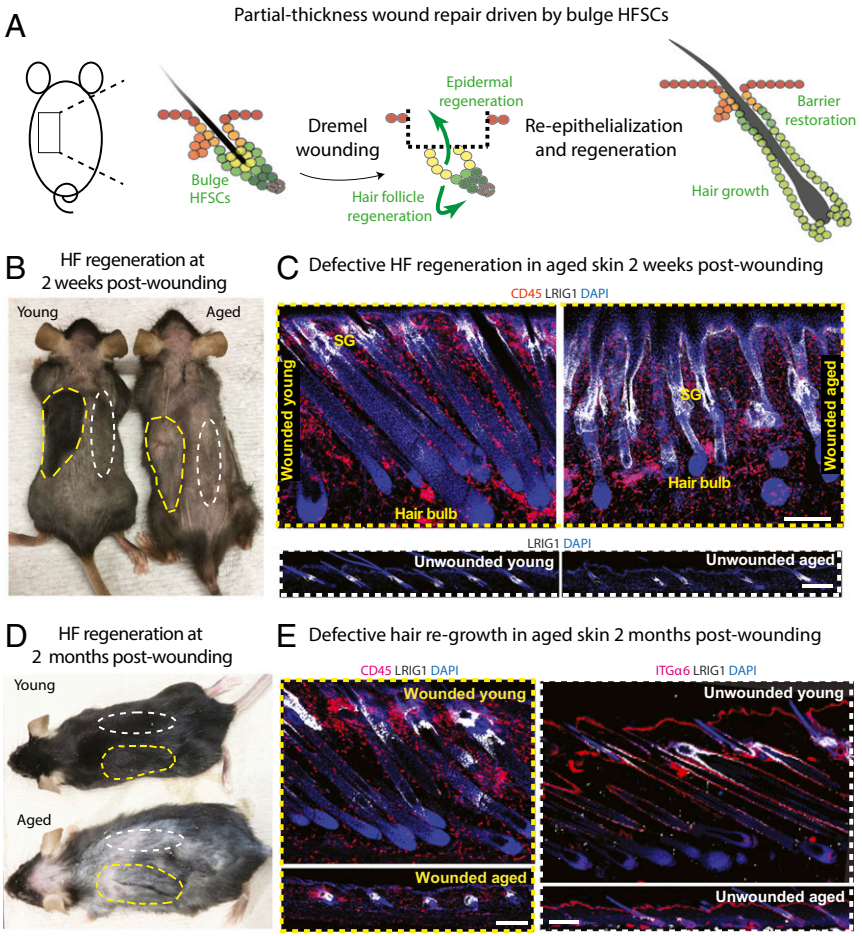

Fig. 5. Age-related deficiency in hair coat recovery following wounding. (*A*) Partial-thickness wound repair model used to challenge telogen-phase bulge HFSCs to re-epithelialize the epidermis and initiate HF regeneration. A dremel tool was used to remove the skin directly above the HF bulges. (*B* and *D*) Photos of mice at either 2 wk (*B*) or 2 mo (*D*) after shaving and dremel wounding of telogen-phase back skin. Yellow dashed lines denote wounded areas; white dashed lines denote unwounded areas used for controls. (*C* and *E*) Immunofluorescence for LRIG1 (white), which marks the HF isthmus, where sebaceous glands (SG) reside, and CD45 (red), a pan-immune cell marker. Notes: At 2 wk, the wounded skin of young mice has turned black, reflecting melanin pigment in full anagen-phase HFs. Unwounded regions and aged wounded regions remain pale, reflecting telogen-phase HFs. The unwounded sample was taken from the 2-wk or 2-mo postwounding mice, respectively, from the unwounded side of the backskin. Anagen has been induced in both young and aged wounded areas, but downgrowth is delayed/impaired in aged HFs, which appear immature. By 2 mo, the unwounded skin of young mice has entered its normal anagen, and the hair coat has regrown. However, aged wounded areas appear to be in telogen at 2 mo postwounding, despite having activated hair cycling at 2 wk. At least five independent biological replicates were performed for each time point; shown are representative images. (Scale bars, 50 μm.) SG, sebaceous glands, which attach at the isthmus.

HFSCs can execute this program necessary for them to survive outside their native bulge microenvironment (*SI Appendix*, Fig. S4*C*). That said, and consistent with previous observations on aged mouse (46) and human keratinocytes (65), colony forming efficiency was diminished in the aged HFSC population (*SI Appendix*, Fig. S4*C*). HFSCs that did adapt to culture conditions, however, formed healthy colonies able to self-renew and give rise to colonies on secondary passaging. After a few passages, colony formation efficiencies became comparable between young and aged HFSCs (*SI Appendix*, Fig. S4*C*). Taken together, these observations suggested that although intrinsic differences exist between young and aged HFSCs, they do not persist in culture media in vitro that is rich in serum and growth factors.

Aged HFSCs Can Be Rejuvenated by Neonatal Dermis during In Vivo Transplantation. Our culture studies suggested that growth-promoting microenvironments might override intrinsic age-related deficiencies in at least some HFSCs within the population. To evaluate the fitness of the aging HFSC population as a whole, and in a physiological context, we turned to HFSC engraftment studies. Previous studies on young skin showed that following culture, HFSCs can regenerate epidermis and HFs when they are combined with freshly isolated neonatal dermal cells and then engrafted onto the back skins of immune-deficient recipient mice (39, 64, 66–69). We were concerned that culture might artificially select for HFSCs most able to withstand culture stress, hence confounding age-related differences. To circumvent this caveat, we omitted the culture step, and performed the engraftments with FACS-purified HFSCs freshly isolated from aged and young skins (Fig. 7*A*; see *Materials and Methods* for further details).

Remarkably, when engrafted with neonatal dermal cells, both young and aged HFSCs generated hairs efficiently on hairless *Nude* mice recipients (Fig. 7*B*). Whole-mount imaging of these grafts further revealed the presence of numerous HFs that formed from both young and aged HFSCs (Fig. 7 *C* and *D* and *SI Appendix*, Fig. S5). In contrast, neither young nor aged HFSCs regenerated hairs or HFs when engrafted with cells from aged skin dermis (Fig. 7 *B* and *D*). Taken together, these observations provide compelling support for the view that the aged skin microenvironment is a major impediment to stem cell activity. Moreover, they demonstrate that neonatal dermis can override the intrinsic age-related differences in hair growth, and rejuvenate aged HFSCs to their youthful behavior.

Discussion

In their Resting State, Aged Bulge HFSCs Maintain their Identity. Our earlier work revealed that in response to a wound, HFSCs from young mice enter a plasticity state known as lineage infidelity, in which they survive by coexpressing dual markers of HF and epidermal identity genes during the healing process (35). Once HFSCs have re-epithelialized the epidermis, they resolve lineage infidelity and thereafter adopt the identity of SCs in their new niche, in this case epidermis.

It had been reported that in aging, bulge SCs ectopically express epidermal genes in the absence of wounding (48). However, this conclusion was based on lineage tracing of progeny marked by *Krt15-promoter*–driven *CrePGR*, which in younger mice is known to exhibit some promiscuity (32, 70) and in older mice could become even more pronounced. Additionally, the prior study used hair-depilation (48), evoking a wound-like response

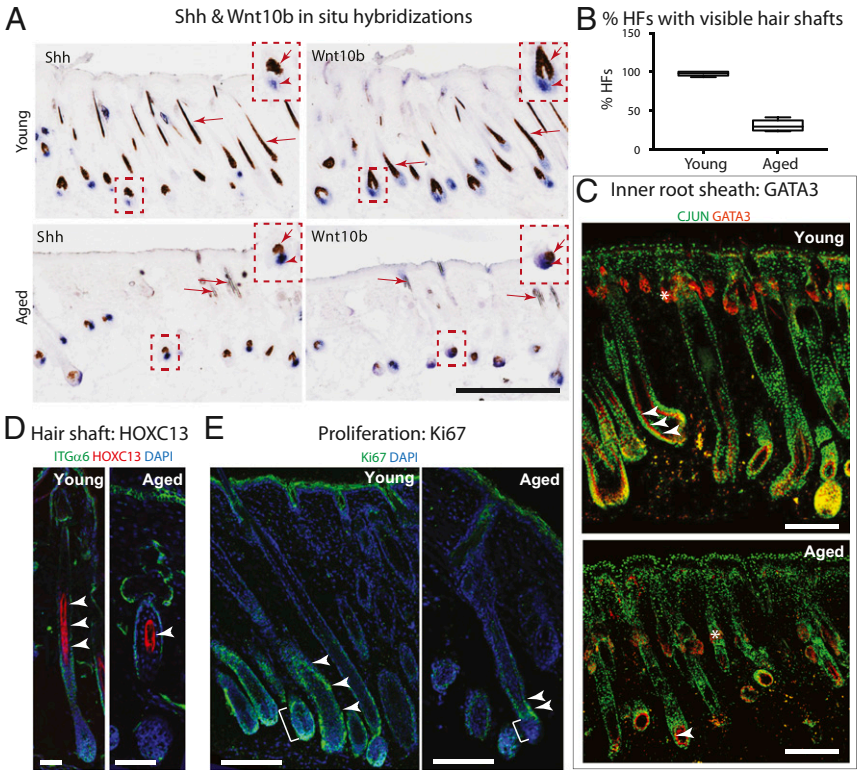

Fig. 6. Defective HF regeneration following wounding in aged skin. (*A*) In situ hybridizations of skin sections processed at 7 d postdremel-wounding of young and aged mice. *Shh* and *Wnt10b* (blue, in situ hybridization signals) are expressed by HFSC progenitors that form at the start of the hair cycle and persist in the hair bulb through anagen (arrowheads in *Insets*). Arrows point to hair shaft cells, which take up brown melanosome pigment as they differentiate to form the hair shaft. (Scale bar, 200 μm.) (*B*) Quantifications showing markedly reduced visible (pigmented) hair shafts in wound-stimulated regions of aged versus young mice. (*C* and *D*) Immunofluorescence for inner root sheath marker GATA3 (*C*, arrowheads) and hair shaft marker HOXC13 (*D*, arrowheads) revealing their reduced numbers if wound-induced HFs in aged compared to young mice (2 wk postdremel-wounding). Notes: AP-1 (CJUN) in green marks the entire skin epithelium during wound repair. An asterisk denotes nonspecific binding. (*E*) Immunofluorescence for proliferation marker Ki67 shows reduced proliferation of short-lived HFSC progenitors within the lower outer root sheath (arrowheads) and the hair bulb (brackets) of wound-induced HFs in aged compared to young mice (2 wk postdremel-wounding). For *C*–*E*, at least five independent biological replicates were analyzed; shown are representative images. (Scale bars, 50 μm.)

(71) that may have contributed to the lineage infidelity that these authors describe. Indeed, lineage infidelity is a natural survival mechanism of wounded skin in younger mice.

Finally, it is important to consider that our transcriptomic analyses here focused only on viable basal progenitors, and any terminally differentiated inner bulge cells that might have undergone signs of fate switching would not have been captured in the scRNA-seq analysis here. That said, our transcriptional profiling by scRNA-seq, as well as immunofluorescence microscopy, showed that although aged HFSCs in balding skin regions were reduced in numbers and activity during the resting stage of the hair cycle, they maintained their HFSC identity within the bulge. In the future, it will be interesting to explore in greater detail the temporal roots of the age-associated decline in HFSC function and to determine whether these age-related changes occur gradually or acutely in the life of the animal. It will also be interesting to explore in greater detail the types of environmental assaults that induce lineage infidelity both in young and in aged animals. Such analysis will likely provide further insights into how bulge HFSCs are altered during aging.

Structural Alterations of Bulge during Aging. In resting (telogen-phase) aged HFs, the structural perturbations to the bulge niche were striking. In younger mice, at the end of each hair cycle, a new bulge niche emerges that maintains contact with DP and fuels the next hair cycle (25). HFs from younger mice can display up to four bulges, but as they exfoliate their old club hair, a hairless bulge will merge with younger bulges to preserve its remaining HFSCs (25). In contrast to younger HFs, however, 2-y-old HFs were mostly left with a single bulge. Interestingly, this feature has been previously observed upon repetitive hair plucking of younger mice (72), leading us to posit that a decline in the ability to anchor the club hair may be contributing to bulge structure collapse in aging mice.

The marked age-related changes in ECM (matrisome) transcripts were intriguing in light of the alterations in bulge structure that we observed. They were also interesting in light of previous findings that *E-Cadherin* (73) and *Col17a1* (48) likely function in maintaining the structure and shape of the bulge. Of interest, it has been reported that in *Caenorhabditis elegans*, the ECM—and in particular collagens—are the key regulators of aging, downstream of insulin/IGF1 signaling and NRF2 transcriptional activity (74). In addition, ECM is also altered during human skin aging (75), suggesting that this could be a conserved pathway modulating organismal aging.

The structural defects in the HFSC niche during natural aging were also interesting in light of prior mouse models where quiescence-governing SC transcription factors were genetically deleted from HFSCs, resulting in a markedly shortened resting phase between hair cycles, and eventual exhaustion of HFSCs in young mice (56, 57). Here we found that naturally aged bulge HFSCs in balding skin regions maintain quiescence and may be inert, consistent with prior studies on aged hairy skin, showing that the resting phase of the hair cycle increases with age, in part due to increased stromal BMP levels (46). *Nfatc1* transcription was not significantly changed in the aged bulge of balding skin, in agreement with prior reports (57). On the other hand, NFATc1 levels, implicated downstream of elevated BMP signaling, are sensitive to posttranscriptional or posttranslational modifications and could contribute to the aging quiescent phenotype, in balding and hairy aged skin.

Changes in the Niche Components and in their Communications with HFSCs. Many of the age-related changes in niche components that we identified are known to influence HFSC behavior in younger animals (18, 19, 22). Although beyond the scope of the present study, our transcriptional analyses revealed insights into how these changes might come about. Notably, in addition to changes in ECM transcripts, age-related changes in HFSC transcripts encoding cell surface signaling molecules were prominent. In this regard, the elevated levels of *Wif1*, encoding a potent WNT inhibitor, were intriguing given the established importance of WNT-signaling in triggering the hair cycle (76, 77). Aged HFSCs

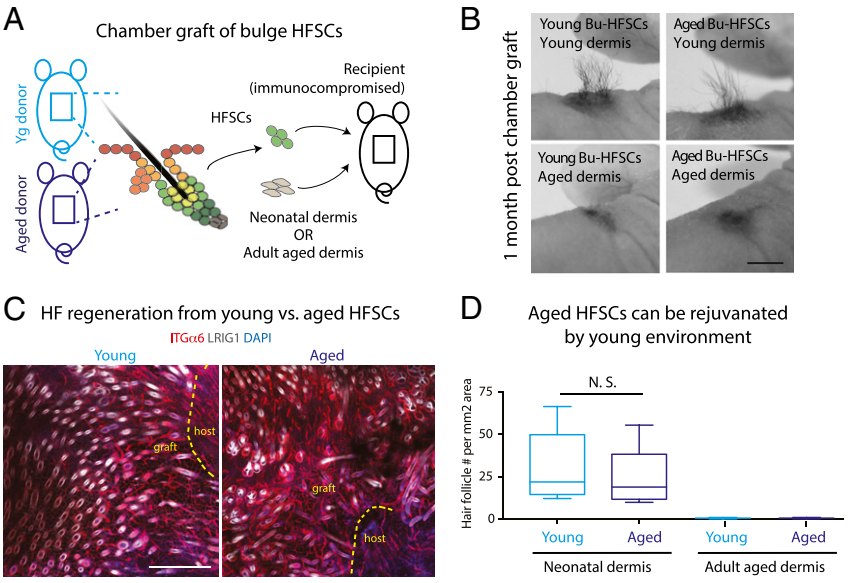

Fig. 7. Tissue microenvironment overrides stem cell intrinsic differences and rejuvenates aged HFSCs. (*A*) Schematics illustrating chamber graft assays, where a small area of skin is removed from the recipient *Nude* mouse back skin and grafted with bulge HFSCs mixed with dermal cells within a domed chamber (chamber graft; see *Materials and Methods*). This method is used to analyze HF regeneration from HFSCs in vivo (39). (*B*–*D*) Photos (*B*) whole-mount immunofluorescence microscopy (*C*), and quantifications (*D*) of grafted young or aged donor HFSCs, combined with either neonatal dermal cells (*B* and *D*) or aged dermal cells (*D*). Note that both aged and young HFSCs produced visible hairs and HFs when grafted with neonatal dermal cells, but failed to do so with aged dermal cells. Immunolabeling of LRIG1 marks HF isthmus in white, and that of INTEGRIN α6 (ITGα6) outlines HFs (also blood vessels) in red. Dashed lines delineate graft and host boundaries. At least five independent biological replicates were performed; shown are representative images. (Scale bars, 1 cm in *B*; 100 μm in *C*.) Paired *t* tests were performed for quantifications (*D*). Data are presented as mean ± SEM. $n = 5$. N.S., not significant.

also showed elevated levels of *Bdnf1* transcripts, encoding a neurotrophic and chemotactic factor for neurons (58), which might account for the mis-positioning of the sensory neurons from the zone above the bulge to the bulge itself. Similarly, the changes in ECM genes, including nephronectin (*Npnt*), could be relevant to the disorganization of APMs, given the previously identified nephronectin:integrin axis as a key communication network in anchoring the APM to the bulge niche (18).

Our finding that Tregs are reduced in aged skin adds yet another player to the growing list of age-related changes in both innate and adaptive immune cells in skin (78, 79). Some of these age-related changes in the HF and its niche share similarities with those that occur in disease-related alopecias, where both HF miniaturization and reduction in Tregs have been reported (80).

In the future, it will be interesting to explore the mechanisms that underlie the perturbed niche microenvironment and altered HFSC-niche cross-talk that we've unearthed here. As the field unravels the complexities involved, the potential mechanistic and molecular similarities between pathological conditions, such as different alopecias and those arising during the natural aging process, should continue to unfold.

Tissue Microenvironment Overrides SC Intrinsic Differences and Rejuvenates Aged HFSCs. Both SC intrinsic (53, 81–84) and tissue microenvironment (46, 47, 85–88) have been shown to regulate SC activity during aging in many tissues, including skin. The age-related differences in colony forming efficiency, seen in freshly isolated HFSCs, did not persist after serial passaging HFSCs in culture. In this regard, it was remarkable that neonatal dermal cells overrode these intrinsic age-related differences in HFSCs and rejuvenated the capacity of aged HFSCs to regenerate HFs in transplantation assays (Fig. 7). This is in contrast to endogenous wound repair, where aged HFSCs faced an aged microenvironment, and both reacted to injury. In this situation, aged HFSCs exhibited clear difficulty in regenerating the hair coat. Since HFSCs are at the helm of the hair regeneration process, their diminished function reduced the pools of all of the short-lived progenitors in the hair lineage. In the future, it will be interesting to examine whether such defects are associated with HFSC intrinsic alterations in the ECM, proliferative potential, or terminal differentiation.

As striking was the failure of aged dermis to support HF regeneration even when young HFSCs were used in transplantation assays. While further studies will be needed to identify the major dermal contributors to the age-related decline in supporting HFSCs (68), our findings underscore the impact of the niche environment on HFSC behavior. In this regard, it is notable that the diminished functional recovery that occurs in the skin after nerve injury can be rejuvenated by a youthful microenvironment (89).

Despite the remarkable effects of a youthful microenvironment, it was not a panacea to revive all of the changes we observed in the aging behavior of HFSCs. In particular, aged HFSCs combined with young stroma still produced follicles whose niche architecture displayed structural abnormalities. Although beyond the current scope, this raised the possibility that self-renewal and regeneration might be more quickly compromised upon serial transplantation and other types of regenerative challenges.

In closing, it is worth returning to our initial finding that aged HFSCs were able to maintain lineage identity. Our findings that aged HFSCs are preserved over a lifetime, and that they can be functionally rescued by supplying exogenous stimuli, provide promising new avenues for regenerative and geriatric medicine. Research aimed at identifying and correcting the key aging dermal component that impedes HFSC behavior could provide viable therapeutic opportunities to treat senile alopecia and to promote healthy aging and wound repair.

Materials and Methods

Mice. Aged (24-mo-old) C57BL/6 animals were obtained from the National Institute on Aging aged rodent colony, and young (2-mo-old) C57BL/6 animals were obtained from Charles River (strain 027). When requesting aged animals, we specified animals with "good hair coats" for the "hairy" aged group with least hair loss, or with "severe baldness" for the "bald" aged group with most hair loss. In the current work, we primarily focused on bald aged mice for analysis except for wherever specified as "hairy" versus "bald." We used female mice to avoid adverse fighting behaviors that would otherwise confound unwounded and wounded skin analysis. All animals were maintained in an American Association for the Accreditation of Laboratory Animal Care Internationally approved Comparative Bio-Science Center at The Rockefeller University and procedures were performed using Institutional Animal Care and Use Committee-approved protocols that adhere to the standards of the National Institutes of Health.

Partial-Thickness Wounding and Chamber Grafts. Partial-thickness wounding (35) and chamber grafts (66) was performed as previously described. Briefly, for chamber grafts, 20 M dermal cells were mixed with 200 K FACS-sorted fresh HFSCs from young or aged back skin and grafted into a silicon chamber implanted onto the back of an anesthetized nude mouse. After 1 wk,

wounds had healed, and chambers were removed. Hair typically appeared 1 to ~2 wk thereafter.

Flow Cytometry of Skin Epithelial and Immune Cells. Preparation of mice back skins for isolation of HFSCs and staining protocols were done as previously described (35). Skin immune cells were analyzed as described previously (90). Antibodies used were: CD34_eFluor660 (1:100; eBioscience 50-0341-80), IntA6_PE (1:100; BD Bioscience 551129), Sca1_PerCP-Cy5.5 (1:1,000; eBioscience 45-5981-80), CD140a_PE-Cy7(1:100; eBioscience 14-1401-81), CD31_PE-Cy7 (1:1,000; eBioscience 25-0311-81), CD117_PE-Cy7 (1:1,000; eBioscience 25-1171-82), CD45_APC-eFluor450(1:1,000; eBioscience 48-0451-80), TCRβ-PercpCy5.5 (1:200; Biolegend), CD4-PE-Cy7 (1:200; Biolegend), CD8-APC-Cy7 (1:200; Biolegend), CD25-BV421 (1:200; Biolegend), Foxp3-FITC (1:100; eBioscience), γδTCR-APC (1:400; Biolegend), Ly6c-FITC (1:500; Biolegend), Ly6g-PE (1:500; Biolegend), CD11c-PE-Cy7 (1:200; Biolegend), CD11b-BV421 (1:1,000; Biolegend), MHCII-AF700 (1:300; Biolegend), CD45-AF700 (1:200; Biolegend), CD64-BV605 (1:200; Biolegend), MerTK-APC (1:100; Biolegend). Dead cells were excluded using LIVE/DEAD Fixable Blue Dead Cell Stain Kit for UV excitation (immune) or using DAPI (epithelial). Sorting was performed on a BD FACSAria II equipped with Diva software (BD Biosciences) at The Rockefeller University's FACS core. Analyses were performed on LSRII FACS analyzers and FlowJo.

scRNA-seq and Analysis. Mice back skin was dissected and digested as described above, and subjected to FACS sorting for live ($DAPI^-$), Lineage-negative ($CD31^-CD45^-CD140A^-CD117^-$), and $ITGA6^+$ subsets. Single-cell libraries were generated on sorted cells using 10X Genomics platform according to the manufacturer's protocol, using 4,000 cells each sample. Data normalization, unsupervised cell clustering and differential expression were carried out using the Seurat R package. The scripts used for analysis and figure generation are available at https://github.com/nyuhuyang/scRNAseq-MouseSkinEpithelia.

Bulk RNA-seq and qPCR. Mouse back skin was prepared as described above, and subjected to FACS sorting for bulge HFSCs ($Lineage^-ITGA6^{high}CD34^+Sca1^-$) or EpdSCs ($Lineage^-ITGA6^{high}CD34^-Sca1^+$), followed by bulk RNA-seq, as previously described (46). Raw data mapping and analysis was performed as previously described (46). qRT-PCR was performed as previously described (35, 91). For differential gene-expression analysis, genes with absolute $\log_2$ fold-change >2 and false-discovery rate <0.05 were considered to be significantly different between two groups under comparison.

ATAC-seq and Analysis. Mice back skin was prepared similar to bulk RNA-seq above, followed by ATAC-seq library prep as previously described (35). Briefly, 100 K freshly FACS-sorted single cells were subjected to Tn5 tagmentation and ATAC libraries were sequenced on HiSeq2500 at The Rockefeller University shared Genomics Resource Center core facility. Library mapping was performed as previously described (35).

Immunofluorescence and In Situ Hybridization. Immunofluorescence on cross-sections (46) or on whole-mount tissues (28, 56) was performed as previously described. The antibodies (and their dilutions) used were as follows: CD34 (rat, 1:100; Pharmingen), GFP (chicken, 1:500; Abcam), Ki67 (sheep, 1:500, R&D systems), Keratin 5 (guinea pig, 1:500; laboratory of E.F.), Keratin 10 (rabbit, 1:500; Covance), LRIG1 (goat, 1:100; R&D Systems), KLF5 (goat, 1:100; R&D Systems), SOX9 (rabbit, 1:500; Millipore), FOXP3 (rat FJK-16s, 1:20; eBioscience). In situ hybridization was performed as previously described (92). Next, 14-μm sections were fixed with 4% PFA, followed by PBS wash, acetylation, and hybridized at 68 °C for 16 h by applying 1 μg/mL of probe. Imaging was performed on Zeiss Axioplan 2, Zeiss Apotome, and Zeiss Inverted LSM 780 laser-scanning confocal microscopes. Figures were prepared using ImageJ, Adobe Photoshop, and Illustrator CS5.

Cell Culture. Colony formation assay was performed as previously described (46). Briefly, FACS-sorted HFSCs were plated in equal number onto Mitomycin C-treated dermal fibroblasts for short term (14 d) in culture. Then cells were fixed, stained with 1% (wt/vol) Rhodamine B, and colony numbers were counted. For long-term passaging, six colonies were individually cloned and grown for 20 passages.

Statistics. Prism7 software was used for statistics analysis, with appropriate methods described in figure legends, and significance was accepted at the 0.05 level of confidence. Briefly, a Student *t* test was used to determine the difference between two groups. To describe the entire population without assumptions about the statistical distribution, box-and-whisker plots are used.

Data Availability. The raw sequencing data have been deposited in the Gene Expression Omnibus database, https://www.ncbi.nlm.nih.gov/geo/ (accession no. GSE124901).

ACKNOWLEDGMENTS. We thank the The Rockefeller University flow cytometry resource center (Svetlana Mazel, director), genomics resource center (Connie Zhao, director) and microscopy resource center (Alison North, director) and the American Association for the Accreditation of Laboratory Animal Care-accredited comparative biology center (R. Tolwani, director) for their services; K.L., L.L., K.S., J.R., E.W., M.S., and J.L. for technical assistance; and S.E., R.A., M.L. and S.L. for critical comments and discussions. Y.G. is supported by the National Institute of Arthritis and Musculoskeletal and Skin Diseases, The Irene Diamond Fund/American Federation for Aging Research Postdoctoral Transition Awards in Aging, Cancer Prevention and Research Institute of Texas first-time recruitment award. E.F. is an HHMI investigator. This work was funded by the Glenn Foundation (E.F.), National Institute of Arthritis and Musculoskeletal and Skin Diseases Grant R01-AR050452 (to E.F.), American Federation for Aging Research (Y.G.), Career Development Award 1K01AR072132-01A1 (to Y.G.), and Cancer Prevention and Research Institute of Texas Recruitment Award FP00006955 (to Y.G.).

1. J. E. Till, E. A. McCulloch, A direct measurement of the radiation sensitivity of normal mouse bone marrow cells. *Radiat. Res.* **14**, 213–222 (1961).
2. A. J. Becker, E. A. McCulloch, J. E. Till, Cytological demonstration of the clonal nature of spleen colonies derived from transplanted mouse marrow cells. *Nature* **197**, 452–454 (1963).
3. N. E. Sharpless, R. A. DePinho, How stem cells age and why this makes us grow old. *Nat. Rev. Mol. Cell Biol.* **8**, 703–713 (2007).
4. D. J. Rossi, C. H. Jamieson, I. L. Weissman, Stems cells and the pathways to aging and cancer. *Cell* **132**, 681–696 (2008).
5. R. A. Signer, S. J. Morrison, Mechanisms that regulate stem cell aging and life span. *Cell Stem Cell* **12**, 152–165 (2013).
6. J. Oh, Y. D. Lee, A. J. Wagers, Stem cell aging: Mechanisms, regulators and therapeutic opportunities. *Nat. Med.* **20**, 870–880 (2014).
7. M. A. Goodell, T. A. Rando, Stem cells and healthy aging. *Science* **350**, 1199–1204 (2015).
8. N. S. Chandel, H. Jasper, T. T. Ho, E. Passegué, Metabolic regulation of stem cell function in tissue homeostasis and organismal ageing. *Nat. Cell Biol.* **18**, 823–832 (2016).
9. M. Lei, C. M. Chuong, STEM CELLS. Aging, alopecia, and stem cells. *Science* **351**, 559–560 (2016).
10. A. Brunet, T. A. Rando, Interaction between epigenetic and metabolism in aging stem cells. *Curr. Opin. Cell Biol.* **45**, 1–7 (2017).
11. B. E. Keyes, E. Fuchs, Stem cells: Aging and transcriptional fingerprints. *J. Cell Biol.* **217**, 79–92 (2018).
12. G. Cotsarelis, Epithelial stem cells: A folliculocentric view. *J. Invest. Dermatol.* **126**, 1459–1468 (2006).
13. K. Kretzschmar, F. M. Watt, Markers of epidermal stem cell subpopulations in adult mammalian skin. *Cold Spring Harb. Perspect. Med.* **4**, a013631 (2014).
14. A. Wabik, P. H. Jones, Switching roles: The functional plasticity of adult tissue stem cells. *EMBO J.* **34**, 1164–1179 (2015).
15. K. A. U. Gonzales, E. Fuchs, Skin and its regenerative powers: An alliance between stem cells and their niche. *Dev. Cell* **43**, 387–401 (2017).
16. Y. Ge, E. Fuchs, Stretching the limits: From homeostasis to stem cell plasticity in wound healing and cancer. *Nat. Rev. Genet.* **19**, 311–325 (2018).
17. G. Cotsarelis, T. T. Sun, R. M. Lavker, Label-retaining cells reside in the bulge area of pilosebaceous unit: Implications for follicular stem cells, hair cycle, and skin carcinogenesis. *Cell* **61**, 1329–1337 (1990).
18. H. Fujiwara *et al.*, The basement membrane of hair follicle stem cells is a muscle cell niche. *Cell* **144**, 577–589 (2011).
19. I. Brownell, E. Guevara, C. B. Bai, C. A. Loomis, A. L. Joyner, Nerve-derived sonic hedgehog defines a niche for hair follicle stem cells capable of becoming epidermal stem cells. *Cell Stem Cell* **8**, 552–565 (2011).
20. E. Festa *et al.*, Adipocyte lineage cells contribute to the skin stem cell niche to drive hair cycling. *Cell* **146**, 761–771 (2011).
21. R. R. Driskell *et al.*, Distinct fibroblast lineages determine dermal architecture in skin development and repair. *Nature* **504**, 277–281 (2013).
22. N. Ali *et al.*, Regulatory T cells in skin facilitate epithelial stem cell differentiation. *Cell* **169**, 1119–1129.e11 (2017).
23. B. A. Shook *et al.*, Myofibroblast proliferation and heterogeneity are supported by macrophages during skin repair. *Science* **362**, eaar2971 (2018).
24. M. C. Salzer *et al.*, Identity noise and adipogenic traits characterize dermal fibroblast aging. *Cell* **175**, 1575–1590 e22 (2018).
25. Y. C. Hsu, H. A. Pasolli, E. Fuchs, Dynamics between stem cells, niche, and progeny in the hair follicle. *Cell* **144**, 92–105 (2011).
26. Y. C. Hsu, L. Li, E. Fuchs, Transit-amplifying cells orchestrate stem cell activity and tissue regeneration. *Cell* **157**, 935–949 (2014).

27. M. Rendl, L. Lewis, E. Fuchs, Molecular dissection of mesenchymal-epithelial interactions in the hair follicle. *PLoS Biol.* **3**, e331 (2005).
28. S. Gur-Cohen *et al*., Stem cell-driven lymphatic remodeling coordinates tissue regeneration. *Science* **366**, 1218–1225 (2019).
29. D. Peña-Jimenez *et al*., Lymphatic vessels interact dynamically with the hair follicle stem cell niche during skin regeneration in vivo. *EMBO J.* **38**, e101688 (2019).
30. G. Taylor, M. S. Lehrer, P. J. Jensen, T. T. Sun, R. M. Lavker, Involvement of follicular stem cells in forming not only the follicle but also the epidermis. *Cell* **102**, 451–461 (2000).
31. M. Ito *et al*., Stem cells in the hair follicle bulge contribute to wound repair but not to homeostasis of the epidermis. *Nat. Med.* **11**, 1351–1354 (2005).
32. V. Levy, C. Lindon, Y. Zheng, B. D. Harfe, B. A. Morgan, Epidermal stem cells arise from the hair follicle after wounding. *FASEB J.* **21**, 1358–1366 (2007).
33. H. J. Snippert *et al*., Lgr6 marks stem cells in the hair follicle that generate all cell lineages of the skin. *Science* **327**, 1385–1389 (2010).
34. M. E. Page, P. Lombard, F. Ng, B. Gottgens, K. B. Jensen, The epidermis comprises autonomous compartments maintained by distinct stem cell populations. *Cell Stem Cell* **13**, 471–482 (2013).
35. Y. Ge *et al*., Stem cell lineage infidelity drives wound repair and cancer. *Cell* **169**, 636–650.e14 (2017).
36. S. Park *et al*., Tissue-scale coordination of cellular behaviour promotes epidermal wound repair in live mice. *Nat. Cell Biol.* **19**, 155–163 (2017).
37. M. Aragona *et al*., Defining stem cell dynamics and migration during wound healing in mouse skin epidermis. *Nat. Commun.* **8**, 14684 (2017).
38. V. Horsley *et al*., Blimp1 defines a progenitor population that governs cellular input to the sebaceous gland. *Cell* **126**, 597–609 (2006).
39. C. Blanpain, W. E. Lowry, A. Geoghegan, L. Polak, E. Fuchs, Self-renewal, multipotency, and the existence of two cell populations within an epithelial stem cell niche. *Cell* **118**, 635–648 (2004).
40. C. Blanpain, E. Fuchs, Stem cell plasticity. Plasticity of epithelial stem cells in tissue regeneration. *Science* **344**, 1242281 (2014).
41. J. Doles, M. Storer, L. Cozzuto, G. Roma, W. M. Keyes, Age-associated inflammation inhibits epidermal stem cell function. *Genes Dev.* **26**, 2144–2153 (2012).
42. B. E. Keyes *et al*., Impaired epidermal to dendritic T cell signaling slows wound repair in aged skin. *Cell* **167**, 1323–1338.e14 (2016).
43. G. Solanas *et al*., Aged stem cells reprogram their daily rhythmic functions to adapt to stress. *Cell* **170**, 678–692.e20 (2017).
44. A. Giangreco, M. Qin, J. E. Pintar, F. M. Watt, Epidermal stem cells are retained in vivo throughout skin aging. *Aging Cell* **7**, 250–259 (2008).
45. R. M. Castilho, C. H. Squarize, L. A. Chodosh, B. O. Williams, J. S. Gutkind, mTOR mediates Wnt-induced epidermal stem cell exhaustion and aging. *Cell Stem Cell* **5**, 279–289 (2009).
46. B. E. Keyes *et al*., Nfatc1 orchestrates aging in hair follicle stem cells. *Proc. Natl. Acad. Sci. U.S.A.* **110**, E4950–E4959 (2013).
47. C. C. Chen *et al*., Regenerative hair waves in aging mice and extra-follicular modulators follistatin, dkk1, and sfrp4. *J. Invest. Dermatol.* **134**, 2086–2096 (2014).
48. H. Matsumura *et al*., Hair follicle aging is driven by transepidermal elimination of stem cells via COL17A1 proteolysis. *Science* **351**, aad4395 (2016).
49. E. Marsh, D. G. Gonzalez, E. A. Lathrop, J. Boucher, V. Greco, Positional stability and membrane occupancy define skin fibroblast homeostasis in vivo. *Cell* **175**, 1620–1633.e13 (2018).
50. S. Mahmoudi *et al*., Heterogeneity in old fibroblasts is linked to variability in reprogramming and wound healing. *Nature* **574**, 553–558 (2019).
51. K. Sudo, H. Ema, Y. Morita, H. Nakauchi, Age-associated characteristics of murine hematopoietic stem cells. *J. Exp. Med.* **192**, 1273–1280 (2000).
52. R. H. Cho, H. B. Sieburg, C. E. Muller-Sieburg, A new mechanism for the aging of hematopoietic stem cells: Aging changes the clonal composition of the stem cell compartment but not individual stem cells. *Blood* **111**, 5553–5561 (2008).
53. I. Beerman *et al*., Functionally distinct hematopoietic stem cells modulate hematopoietic lineage potential during aging by a mechanism of clonal expansion. *Proc. Natl. Acad. Sci. U.S.A.* **107**, 5465–5470 (2010).
54. K. Nalapareddy *et al*., Canonical Wnt signaling ameliorates aging of intestinal stem cells. *Cell Rep.* **18**, 2608–2621 (2017).
55. S. Müller-Röver *et al*., A comprehensive guide for the accurate classification of murine hair follicles in distinct hair cycle stages. *J. Invest. Dermatol.* **117**, 3–15 (2001).
56. K. Lay, T. Kume, E. Fuchs, FOXC1 maintains the hair follicle stem cell niche and governs stem cell quiescence to preserve long-term tissue-regenerating potential. *Proc. Natl. Acad. Sci. U.S.A.* **113**, E1506–E1515 (2016).
57. L. Wang, J. A. Siegenthaler, R. D. Dowell, R. Yi, Foxc1 reinforces quiescence in self-renewing hair follicle stem cells. *Science* **351**, 613–617 (2016).
58. J. Leibrock *et al*., Molecular cloning and expression of brain-derived neurotrophic factor. *Nature* **341**, 149–152 (1989).
59. D. M. Waldera Lupa *et al*., Characterization of skin aging-associated secreted proteins (SAASP) produced by dermal fibroblasts isolated from intrinsically aged human skin. *J. Invest. Dermatol.* **135**, 1954–1968 (2015).
60. B. St-Jacques *et al*., Sonic hedgehog signaling is essential for hair development. *Curr. Biol.* **8**, 1058–1068 (1998).
61. H. Yang, R. C. Adam, Y. Ge, Z. L. Hua, E. Fuchs, Epithelial-mesenchymal micro-niches govern stem cell lineage choices. *Cell* **169**, 483–496.e13 (2017).
62. N. M. Joseph, S. J. Morrison, Toward an understanding of the physiological function of mammalian stem cells. *Dev. Cell* **9**, 173–183 (2005).
63. R. C. Adam *et al*., Pioneer factors govern super-enhancer dynamics in stem cell plasticity and lineage choice. *Nature* **521**, 366–370 (2015).
64. S. Claudinot, M. Nicolas, H. Oshima, A. Rochat, Y. Barrandon, Long-term renewal of hair follicles from clonogenic multipotent stem cells. *Proc. Natl. Acad. Sci. U.S.A.* **102**, 14677–14682 (2005).
65. Y. Barrandon, H. Green, Three clonal types of keratinocyte with different capacities for multiplication. *Proc. Natl. Acad. Sci. U.S.A.* **84**, 2302–2306 (1987).
66. W. C. Weinberg *et al*., Reconstitution of hair follicle development in vivo: Determination of follicle formation, hair growth, and hair quality by dermal cells. *J. Invest. Dermatol.* **100**, 229–236 (1993).
67. U. Lichti *et al*., In vivo regulation of murine hair growth: Insights from grafting defined cell populations onto nude mice. *J. Invest. Dermatol.* **101** (suppl. 1), 124S–129S (1993).
68. C. A. Collins, K. Kretzschmar, F. M. Watt, Reprogramming adult dermis to a neonatal state through epidermal activation of β-catenin. *Development* **138**, 5189–5199 (2011).
69. M. Lei *et al*., Self-organization process in newborn skin organoid formation inspires strategy to restore hair regeneration of adult cells. *Proc. Natl. Acad. Sci. U.S.A.* **114**, E7101–E7110 (2017).
70. R. J. Morris *et al*., Capturing and profiling adult hair follicle stem cells. *Nat. Biotechnol.* **22**, 411–417 (2004).
71. M. Ito, K. Kizawa, K. Hamada, G. Cotsarelis, Hair follicle stem cells in the lower bulge form the secondary germ, a biochemically distinct but functionally equivalent progenitor cell population, at the termination of catagen. *Differentiation* **72**, 548–557 (2004).
72. T. Chen *et al*., An RNA interference screen uncovers a new molecule in stem cell self-renewal and long-term regeneration. *Nature* **485**, 104–108 (2012).
73. K. Lay *et al*., Stem cells repurpose proliferation to contain a breach in their niche barrier. *eLife* **7**, e41661 (2018).
74. C. Y. Ewald, J. N. Landis, J. Porter Abate, C. T. Murphy, T. K. Blackwell, Dauer-independent insulin/IGF-1-signalling implicates collagen remodelling in longevity. *Nature* **519**, 97–101 (2015).
75. A. Giangreco, S. J. Goldie, V. Failla, G. Saintigny, F. M. Watt, Human skin aging is associated with reduced expression of the stem cell markers beta1 integrin and MCSP. *J. Invest. Dermatol.* **130**, 604–608 (2010).
76. R. DasGupta, E. Fuchs, Multiple roles for activated LEF/TCF transcription complexes during hair follicle development and differentiation. *Development* **126**, 4557–4568 (1999).
77. W. H. Lien *et al*., In vivo transcriptional governance of hair follicle stem cells by canonical Wnt regulators. *Nat. Cell Biol.* **16**, 179–190 (2014).
78. P. J. Linton, K. Dorshkind, Age-related changes in lymphocyte development and function. *Nat. Immunol.* **5**, 133–139 (2004).
79. E. J. Kovacs *et al*., Aging and innate immunity in the mouse: Impact of intrinsic and extrinsic factors. *Trends Immunol.* **30**, 319–324 (2009).
80. L. Petukhova *et al*., Genome-wide association study in alopecia areata implicates both innate and adaptive immunity. *Nature* **466**, 113–117 (2010).
81. D. J. Rossi *et al*., Cell intrinsic alterations underlie hematopoietic stem cell aging. *Proc. Natl. Acad. Sci. U.S.A.* **102**, 9194–9199 (2005).
82. J. Flach *et al*., Replication stress is a potent driver of functional decline in ageing haematopoietic stem cells. *Nature* **512**, 198–202 (2014).
83. D. Sun *et al*., Epigenomic profiling of young and aged HSCs reveals concerted changes during aging that reinforce self-renewal. *Cell Stem Cell* **14**, 673–688 (2014).
84. B. D. Cosgrove *et al*., Rejuvenation of the muscle stem cell population restores strength to injured aged muscles. *Nat. Med.* **20**, 255–264 (2014).
85. I. M. Conboy *et al*., Rejuvenation of aged progenitor cells by exposure to a young systemic environment. *Nature* **433**, 760–764 (2005).
86. L. Katsimpardi *et al*., Vascular and neurogenic rejuvenation of the aging mouse brain by young systemic factors. *Science* **344**, 630–634 (2014).
87. M. Sinha *et al*., Restoring systemic GDF11 levels reverses age-related dysfunction in mouse skeletal muscle. *Science* **344**, 649–652 (2014).
88. G. Kalamakis *et al*., Quiescence modulates stem cell maintenance and regenerative capacity in the aging brain. *Cell* **176**, 1407–1419.e14 (2019).
89. M. W. Painter *et al*., Diminished Schwann cell repair responses underlie age-associated impaired axonal regeneration. *Neuron* **83**, 331–343 (2014).
90. S. Naik *et al*., Inflammatory memory sensitizes skin epithelial stem cells to tissue damage. *Nature* **550**, 475–480 (2017).
91. Y. Ge, L. Zhang, M. Nikolova, B. Reva, E. Fuchs, Strand-specific in vivo screen of cancer-associated miRNAs unveils a role for miR-21(*) in SCC progression. *Nat. Cell Biol.* **18**, 111–121 (2016).
92. T. Ouspenskaia, I. Matos, A. F. Mertz, V. F. Fiore, E. Fuchs, WNT-SHH antagonism specifies and expands stem cells prior to niche formation. *Cell* **164**, 156–169 (2016).